

**BIOMARKERS, GENOMICS, PROTEOMICS, AND GENE REGULATION**

Integrated Transcriptomic and Proteomic Analysis Identifies Plasma Biomarkers of Hepatocellular Failure in Alcohol-Associated Hepatitis



Josepmaria Argemi,^{*†} Komal Kedia,[‡] Marina A. Gritsenko,[§] Ana Clemente-Sanchez,^{*¶} Aliya Asghar,^{||} Jose M. Herranz,[†] Zhang-Xu Liu,^{**} Stephen R. Atkinson,^{*} Richard D. Smith,[§] Trina M. Norden-Krichmar,^{††} Le Z. Day,[§] Andrew Stolz,^{**} John A. Tayek,^{‡‡} Ramon Bataller,^{*} Timothy R. Morgan,^{||} Jon M. Jacobs,[§] and the Southern California Alcoholic Hepatitis Consortium and the InTeam Consortium

From the Division of Gastroenterology, Hepatology, and Nutrition,^{*} Department of Medicine, Pittsburgh Liver Research Center, University of Pittsburgh, Pittsburgh, Pennsylvania; the Hepatology Program,[†] Centro de Investigación Médica Aplicada, Liver Unit, Clínica Universidad de Navarra, Instituto de Investigación de Navarra, Universidad de Navarra, Pamplona, Spain; the Department of Pharmacokinetics, Pharmacodynamics and Drug Metabolism,[‡] Merck & Co, Inc., West Point, Pennsylvania; the Biological Sciences Division and Environmental Molecular Sciences Laboratory,[§] Pacific Northwest National Laboratory, Richland, Washington; the Biomedical Research Networking Center in Hepatic and Digestive Diseases,[¶] Instituto de Salud Carlos III, Madrid, Spain; the Gastroenterology Service,^{||} VA Long Beach Healthcare System, Long Beach, California; the Division of Gastrointestinal and Liver Disease,^{**} Department of Medicine, Keck School of Medicine, University of Southern California, Los Angeles, California; the Department of Epidemiology,^{††} School of Medicine, University of California, Irvine, Irvine, California; and the Harbor-University of California, Los Angeles Medical Center,^{‡‡} Torrance, California

Accepted for publication
August 31, 2022.

Address correspondence to
Timothy R. Morgan, M.D., VA
Long Beach Healthcare System
- 11 (Med/GI), 5901 E. Seventh
St., Long Beach, CA 90822; or
Jon M. Jacobs, Ph.D., Envi-
ronmental and Molecular Sci-
ences Laboratory, Pacific
Northwest National Laboratory,
3335 Innovation Blvd., Rich-
land, WA 99354.
E-mail: timothy.morgan@va.gov
or jon.jacobs@pnnl.gov.

Alcohol-associated hepatitis (AH) is a form of liver failure with high short-term mortality. Recent studies have shown that defective function of hepatocyte nuclear factor 4 alpha (HNF4a) and systemic inflammation are major disease drivers of AH. Plasma biomarkers of hepatocyte function could be useful for diagnostic and prognostic purposes. Herein, an integrative analysis of hepatic RNA sequencing and liquid chromatography–tandem mass spectrometry was performed to identify plasma protein signatures for patients with mild and severe AH. Alcohol-related liver disease cirrhosis, nonalcoholic fatty liver disease, and healthy subjects were used as comparator groups. Levels of identified proteins primarily involved in hepatocellular function were decreased in patients with AH, which included hepatokines, clotting factors, complement cascade components, and hepatocyte growth activators. A protein signature of AH disease severity was identified, including thrombin, hepatocyte growth factor α , clusterin, human serum factor H-related protein, and kallistatin, which exhibited large abundance shifts between severe and nonsevere AH. The combination of thrombin and hepatocyte growth factor α discriminated between severe and nonsevere AH with high sensitivity and specificity. These findings were correlated with the liver expression of genes encoding secreted proteins in a similar cohort, finding a highly consistent plasma protein signature reflecting HNF4A and HNF1A functions. This unbiased proteomic-transcriptome analysis identified plasma protein signatures and pathways associated with disease severity, reflecting HNF4A/1A activity useful for diagnostic assessment in AH. (*Am J Pathol* 2022, 192: 1658–1669; <https://doi.org/10.1016/j.ajpath.2022.08.009>)

Supported by the NIH through National Institute of Alcohol Abuse and Alcoholism (NIAAA) grants 1U01AA021886 and U01AA21884 for the Southern California Alcoholic Hepatitis Consortium and U01AA021908 for the InTeam Alcoholic Hepatitis Consortium. Analysis was supported by NIAAA U01 AA021918 (J.M.J.), NIAAA U01 AA021857 (Z.-X.L.), and NIAAA U01 AA021838 (T.M.N.-K.). Portions of this research were also supported by NIH National Institute of General Medical Sciences

GM103493 (R.D.S.) and NIH NIAAA 1R21AA028117 (J.M.J.). J.A. was sponsored by the Agencia Estatal de Salud PI20-01663 and Fundacion Echebano. A.C.-S. was supported by a scholarship grant for study extension abroad, sponsored by the Spanish Association for the Study of the Liver.

R.B. and T.R.M. are equal senior authors.

Disclosures: None declared.

Alcohol-related liver disease (ALD) is the main cause of liver-related mortality worldwide.^{1,2} Although many patients have silent disease, others develop alcohol-related hepatitis (AH), a life-threatening subacute form of liver failure that occurs in the setting of prolonged heavy alcohol use in patients with underlying alcoholic cirrhosis or advanced fibrosis. Severe AH (sAH) presents with jaundice, abnormal clotting function, hepatic encephalopathy, and complications of portal hypertension. Although a histologic prognostic score system can be used,³ transjugular biopsy is not available in most centers, and new noninvasive biomarkers could be useful for patient stratification and treatment allocation in clinical trials. The current standard of care for severe AH (ie, prednisolone) has limited efficacy and does not prolong survival beyond 28 days.^{4,5} Moreover, up to 30% to 40% of patients do not respond to corticosteroids, and their 6-month mortality can exceed 60%.^{6,7} The development of novel targeted therapies represents an urgent need in clinical hepatology.

Impaired function of liver-enriched transcription factors (LETFs), such as hepatocyte nuclear factor 4 alpha (HNF4a)/HNF1a, as well as systemic inflammatory response syndrome are key drivers of liver and subsequent multiorgan failure in patients with severe AH.^{8,9} Identification of plasma biomarkers that reflect impaired hepatic function and/or systemic inflammation may have prognostic value and can favor precision medicine. To achieve this goal, global proteome analysis of blood plasma has been highly informative across multiple clinical conditions.^{10–13} Current mass spectrometry techniques provide exceptional sensitivity and quantification toward understanding the network of protein pathways, secretion systems, and responses to stimuli.^{14,15} Herein, this approach was used to provide a novel comprehensive study of plasma proteome in a large cohort of patients with ALD, including AH, and suggest specific markers associated to AH severity. An unbiased identification of specific plasma signatures of hepatocellular failure in patients with AH was obtained, revealing key proteins associated with severity and providing a novel noninvasive molecular tool for clinical and research purposes.

Materials and Methods

Study Population

Plasma samples from patients with AH were obtained by the human biorepositories of the National Institute of Alcohol Abuse and Alcoholism—funded Southern California Alcoholic Hepatitis Consortium and the InTeam Consortium. The diagnosis of AH was established following the National Institute of Alcohol Abuse and Alcoholism guidelines.¹⁶ All participating clinical sites and analysis sites had approval from their institutional review board before the start of the investigation, and annually thereafter. All patients signed informed consents before providing plasma specimens. A

total of 57 patients with AH were included in the plasma proteome analysis. Plasma was collected from all patients at baseline visit (before starting corticosteroids or other treatment for AH), and patients with AH were stratified on the basis of severity, with severe AH group (biopsy proven and Maddrey discriminant function >32 ; $N = 43$) forming the primary comparison with the control populations. The remaining 14 patients had nonsevere AH (nsAH; Maddrey discriminant function <32). Plasma samples from 49 subjects, including healthy controls ($n = 16$) and those with nonalcoholic fatty liver disease ($n = 11$), were also analyzed. In addition, to study the effects of alcohol intake and chronic alcohol-related liver disease on plasma proteome, patients with ALD and recent alcohol intake (abstinent <30 days; $N = 11$) and abstinent (no alcohol intake >6 months; $N = 11$) were analyzed. **Table 1** shows the clinical characteristics of the study participants.

Proteomics Analysis

Plasma Sample Processing for Proteomics

Blood was collected into EDTA tubes, followed by centrifugation, placement of plasma in cryovials, and freezing at -80°C . Individual human plasma samples were partitioned and depleted of 14 specific highly abundant proteins using a ProteomeLab 12.7 \times 79.0-mm human IgY14 LC10 affinity liquid chromatography column (Beckman Coulter, Fullerton, CA), which was performed using the manufacturer's instructions. Further processing of the flow-through portion of the plasma depletion included automated protein isolation, denaturation, tryptic digestion, and peptide isolation, as previously described.¹⁷ Tandem Mass Tag (TMT) 10 labeling (Thermo Fisher Scientific, Waltham, MA) was performed as dictated by the manufacturer's protocol. A total of 35 μg of peptide was included in each channel with the inclusion of a universal reference in each TMT10 experiment. Each TMT10 multiplexed experiment was subjected to offline high-performance liquid chromatography separation, as previously described,^{14,18} which resulted in a concatenated 12 fractions for each TMT10 experiment.

Liquid Chromatography—Mass Spectrometry Analysis

A PAL autosampler (CTC Analytics AG, Zwingen, Switzerland) equipped with two six-port valves (Valco Instruments Co Inc., Houston, TX) was used for sample injection. After being injected into a 25- μL loop, the sample was concentrated into a solid phase extraction column (150 μm i.d., 360 μm o.d., 4 cm long) at a flow rate of 5 $\mu\text{L}/\text{minute}$. The nano-liquid chromatography column (50 μm i.d., 360 μm o.d., 50 cm long) was packed with 3- μm C18 packing material (300- \AA pore size; Phenomenex, Terrence, CA). Mobile phases (buffer A: 0.1% formic acid in water; and buffer B: 0.1% formic acid in acetonitrile) were delivered by a nano-ultra-performance liquid chromatography pump (Dionex UltiMate NCP-3200RS; Thermo Scientific, Waltham, MA) at a flow rate of 150 nL/minute. The liquid

Table 1 Baseline Clinical Parameters for All Patients

Variable	AH: severe SCAHC (n = 23)	AH: severe InTeam (n = 20)	AH: nonsevere (n = 14)	HC (n = 16)	NAFLD (n = 11)	AC: recent (n = 11)	AC: abstinent (n = 11)
Age, years	48 (39 to 56)	55 (48 to 62)	48 (43 to 60)	28 (20 to 54)	47 (36 to 60)	56 (45 to 62)	56 (49 to 62)
Sex, % male	96	80	64	62	72	100	100
Ethnicity, %							
African American	8.7	10	7.2	13	18	0	0
White, Hispanic	61	35	43	31	27	64	82
White, non-Hispanic	30	50	50	0	45	27	18
Asian	0	0	0	38	9	0	0
American Indian Pacific Islander	0	5	0	13	0	0	0
Pacific Islander	0	0	0	0	0	9	0
Total bilirubin, mg/dL	11.9 (7.75 to 15.35)	17.4 (9.8 to 26.15)	5.1 (3.5 to 7.1)	0.5 (0.4 to 0.7)	0.85 (0.7 to 1)	3.6 (1.2 to 5.4)	1.2 (0.85 to 2.1)
AST, IU	115 (91.8 to 149)	126 (83.5 to 157)	127 (103 to 297)	18 (14 to 21.5)	59 (49 to 67.5)	49 (35.8 to 65.5)	39 (27.5 to 46)
ALT, IU	50 (35.5 to 53.5)	50 (29.5 to 66)	38 (32 to 84)	17 (13.5 to 23.5)	95 (64.5 to 114)	32 (26 to 39.5)	25 (19.5 to 14.3)
MELD	22.4 (21.4 to 25.7)	32.8 (30.1 to 35.2)	17.1 (14.4 to 19.0)	6.5 (6 to 7.3)	7 (7 to 7.8)	17 (10.9 to 22.5)	10 (9 to 13.4)
Maddrey DF	51.3 (40.3 to 64.1)	65.9 (45.2 to 95.3)	26.2 (17.8 to 29.5)	0.4 (−1.1 to 4.2)	4.1 (3.5 to 5.1)	33.2 (12.0 to 54.5)	10 (7.25 to 14.3)

Results are presented as median (interquartile range) unless noted otherwise.

AC, alcoholic cirrhotic; AH, alcohol-associated hepatitis; ALT, alanine aminotransferase; AST, aspartate aminotransferase; DF, discriminant function; HC, healthy control; MELD, Model for End-Stage Liver Disease; NAFLD, nonalcoholic fatty liver disease; SCAHC, Southern California Alcoholic Hepatitis Consortium.

chromatography method was programmed as a 100-minute linear gradient from 8% to 22% Buffer B, followed by a 15-minute linear gradient to 45% Buffer B, after which the column was washed with 90% Buffer B for 5 minutes and re-equilibrated with 2% Buffer B for 20 minutes. The separated peptides were analyzed using a Thermo Scientific Q Exactive Plus. Data were acquired in a data-dependent mode with a full mass spectrometry scan from m/z 350 to 1800 at a resolution of 70,000 at m/z 400 with automated gain control setting set to 5×10^5 and maximum ion injection period set to 50 milliseconds. Top 10 precursor ions having intensities $>2.5 \times 10^4$ and charges between 2 and 8 were selected with an isolation window of 2 Da for tandem mass spectrometry sequencing at a high-energy C-trap dissociation energy of 33%. Tandem mass spectrometry spectra were acquired at a resolution of 17,500. The automated gain control target was 1×10^5 , and the maximum ion accumulation time was 200 milliseconds. The dynamic exclusion time was set at 40 seconds.

Proteomics Data Analysis

Liquid chromatography–tandem mass spectrometry raw data were converted into dta files using Bioworks Cluster 3.2 (Thermo Fisher Scientific, Cambridge, MA). The MSGF + algorithm¹⁹ was used to search tandem mass

spectrometry spectra against the Human Uniprot database (Uniprot_SPROT 2017 to 04-12; 20,198 entries). The key search parameters used were 20 ppm tolerance for precursor ion masses, 2.5- and −1.5-Da window on fragment ion mass tolerances, no limit on missed cleavages, partial tryptic search, no exclusion of contaminants, dynamic oxidation of methionine (15.9949 Da), static iodoacetamide alkylation on cysteine (57.0215 Da), and static TMT modification of lysine and N-termini (144.1021 Da). The decoy database searching method^{20,21} was used to control the false discovery rate at the unique peptide level to $<0.01\%$ and subsequent protein level to $<0.1\%$. Quantification was based on initially summing to the protein level the sample-specific peptide reporter ion intensities captured for each channel across all 12 analytical fractions. Final data for statistical analysis was the ratio of each protein summed value with the pooled reference control within each TMT10 experiment to adjust for experiment-specific variability. The mass spectrometry proteomics data have been deposited to the ProteomeXchange Consortium 22 with the data set identifier PXD016117 (<http://proteomecentral.proteomexchange.org/cgi/GetDataset?ID=PX016117>, last accessed September 14, 2022) and MassIVE Accession MSV000084528 (<https://massive.ucsd.edu/ProteoSAFe/static/massive.jsp>, last accessed September 14, 2022).²²

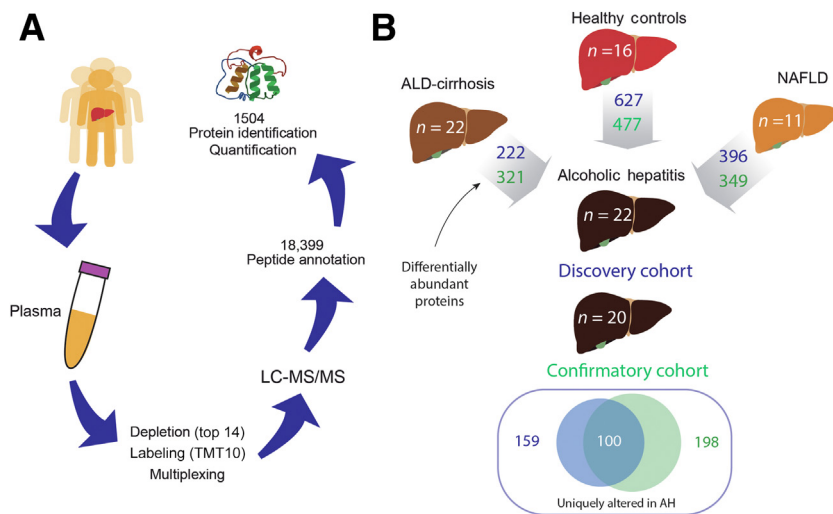


Figure 1 Workflow of the comparison of the study. **A:** For unbiased proteomics, the plasma was depleted from the top 14 most abundant proteins, and peptides were labeled and multiplexed. **B:** Plasma from a total of 90 subjects was analyzed: healthy subjects, patients with nonalcoholic fatty liver disease (NAFLD), patients with advanced alcohol-related liver disease (ALD), and patients with alcoholic hepatitis from two different cohorts, Southern California Alcoholic Hepatitis Consortium (SCAHC) Discovery cohort and InTeam Confirmatory cohort (AH). A total of 100 proteins were uniquely altered in patients with AH when compared with healthy and diseased controls. Blue indicates differentially abundant proteins for Discovery cohort, and green indicates proteins for Confirmatory cohort. $N = 16$ healthy subjects (**B**); $N = 11$ patients with NAFLD (**B**); $N = 22$ patients with ALD (**B**); $N = 42$ patients with AH (**B**). LC-MS/MS, liquid chromatography–tandem mass spectrometry; TMT, Tandem Mass Tag.

Proteomics Statistical and Pathway Analysis

Protein-level TMT ratio abundance values were central tendency normalized and then subjected to statistical comparison between patient populations and time points of interest. Primary comparisons were based on analysis of variance analysis at a <0.05 P -value threshold coupled with a fold change criteria minimum of ± 0.15 between protein ratio abundances. Pathway mapping was performed utilizing Gene Ontology annotations extracted from DAVID version 6.8 (<https://david.ncifcrf.gov>, last accessed March 29, 2021) using the ontology for biological process (GOTERM_BP_DIRECT). Bonferroni correction for only those Gene Ontology term pathways that had a $P < 0.05$ was selected. For inferring general pathways of differential proteome, Cytoscape network analysis was performed (version 3.8.2), where the nodes are gene sets from the Molecular Signatures Data Base (Broad Institute, Cambridge, MA) and the edges are the similarity—overlap—between gene sets. A node cutoff of 0.08 and edge cutoff (similarity) of 0.375 was used for depicting the network with the data analysis.

Liver RNA Sequencing Analysis

RNA sequencing data were obtained from normal livers ($n = 10$) and from biopsies of patients with early silent ALD ($n = 12$), nonsevere AH ($n = 9$), and severe AH ($n = 28$); the processing, sequencing, and clinical data have been described previously,⁹ and the raw data and metadata are publicly available in the Database of Genotypes and Phenotypes of the National Library of Medicine under the accession study code phs001807. v1. p1 (https://www.ncbi.nlm.nih.gov/projects/gap/cgi-bin/study.cgi?study_id=phs001807.v1.p1, last accessed September 22, 2022).

Proteome: Liver RNA Sequencing Integrative Analysis

Using a ranked list with fold ratios and with a threshold false discovery rate of 0.001, Ingenuity Pathway Analysis (Qiagen, Hilden, Germany; version 2019) was used to infer transcription factor signatures. Log fold ratios were used to compare the changes in the liver transcriptome with the changes observed in the plasma proteome. Correlation plots were made to infer the genes coding for secreted proteins using Compartment Data Base.²³ Criteria to define a secreted gene included having as Localization parameter, one of the following: Extracellular space, Extracellular Region, Extracellular region part, and/or Extracellular exosome. To infer the transcription factor target genes in an unbiased manner, the transcription factor category within the C3 collection (Motif) of the Molecular Signatures Data Base was used. For calculating correlation coefficients, *psych* package version 1.9.12 (<https://cran.r-project.org>, last accessed September 22, 2022) was used. Correlation plots, box plots, bar plots, and heat maps were performed using *ggplot2* package. Gene-gene correlation plots were made using *corrplot* package.

Statistical Analysis

After mean-centered normalization, differences of protein abundance between patients with severe and nonsevere AH were compared using t test. Only proteins with $P < 0.01$ were considered for logistic regression analysis. To perform logistic regression, a generalized linear model using each of the top candidates was fitted using *stats* package. Odds ratios were plotted using *ggplots* package. Receiver operating characteristic curves were visualized using *pROC* package. Area under the curve and CIs were calculated using the same package.

Results

Identification of Plasma and Liver-Derived Protein Signatures in AH

In total, 18,399 peptides corresponding to 1504 plasma proteins were uniquely identified and quantified (Figure 1A and Supplemental Table S1). To identify a specific AH proteomic signature, a tiered analysis strategy was executed that incorporated the comparison of severe AH from two different study cohorts together with appropriate healthy and disease control plasma samples. Interestingly, as liver disease progresses both from healthy liver to metabolism-related damage (nonalcoholic fatty liver disease) or alcohol-related liver cirrhosis (ALD), the number of differential plasma proteins decreases, indicating that some components of the differential proteome in AH are shared with other causes of liver damage and with chronic alcohol-associated cirrhosis without AH phenotype (Figure 1B and Supplemental Table S2). In total, an overlapping set of 100 proteins were uniquely altered in patients with severe AH in both cohorts. An unbiased analysis of top differentially abundant proteins included hepatocyte-specific transporters and apolipoproteins, such as hemopexin (*HPX* gene), apolipoprotein C, apolipoprotein A (*LPA* gene), retinol-binding protein 4 (*RBP4* gene), and serum-derived hyaluronan-associated protein, proteins related to coagulation, such as kallikrein B1 or heparin cofactor 2 (*HEP2*; *SERPIND1* gene), and other transport/functional proteins, such as insulin-like growth factor modulators [insulin-like growth factor binding protein 2 (*IBP2*) and insulin-like growth factor-binding protein complex acid labile subunit (*ALS*)], which were down-regulated (Figure 2A). Top up-regulated proteins included immunomodulatory factors, such as complement 7, Golgi membrane protein 1, C-reactive protein, intercellular adhesion molecule 1, and the monocyte surface scavenger C163A (*CD163* gene) (Figure 2A), many of which have been previously investigated.^{8,24–26} Gene Set Enrichment Analysis was used to provide an expanded network, and infer the potential relationship between extracellular matrix–immune system modulators and proteins related to liver dysfunction associated with AH. The driving features of these altered pathways included the down-regulation of the coagulation and complement systems (Figure 2, B and C) and pathways related to cytoskeleton, such as Rho GTPases (Figure 2, B and C) and others (Figure 2, B and C); and the up-regulation of the extracellular matrix and cell-cell interactions (Figure 2, B and C), and the protein glycosylation pathways (Figure 2, B and C) and others (Figure 2, B and C). As expected, when performing protein-protein correlation analysis in plasma of patients with AH, down-regulated liver-specific proteins conversely correlated with up-regulated proinflammatory proteins (Supplemental Figure S1), specifically in each patient with AH, indicating that these two processes are tightly connected in AH. Interestingly, many of the inflammatory mediators, whose origins are probably immune cells, were found progressively

up-regulated on alcohol-mediated damage (Figure 2D and Supplemental Figure S2).

Integrated Analysis of Liver Secretome Expression and Proteome Identifies Biomarkers of Hepatocyte-Enriched Transcription Factor Activation

The main genetic signature revealed in livers of patients with severe AH is the down-regulation of HNF4A-dependent transcription.⁹ The expression of LETFs is also impaired in AH when compared with early-compensated phases of ALD.⁹ Conversely, the activity of other transcription factors, such as STAT3, nuclear factor kappa B subunit 1 (NFkB1), or nuclear factor NF-kappa-B p65 subunit (RELA), is up-regulated in the liver transcriptome of patients with AH.⁹ The study aimed to find the presence of plasmatic noninvasive signatures of transcription factor activity in the liver. After filtering out plasma proteins for which there is no liver gene expression, the overlapping liver gene expression was compared with their respective plasma protein abundance. Interestingly, the changes in whole plasma proteome of patients with AH versus healthy controls were significantly correlated with the changes in the transcriptome of AH livers versus normal livers ($N = 930$; $R = 0.258$; $P = 1.3 \times 10^{-15}$), indicating a driving role of liver dysfunction and protein expression in the plasma proteome (Figure 3A and Supplemental Tables S3 and S4). A transcription factor footprint was then computed from the differentially expressed genes in severe AH when compared with normal livers (Figure 3B) using data previously published.⁹ By using Gene Set Enrichment Analysis and the UniprotDB localization knowledge base, the number of transcription factor–dependent secreted target genes was inferred. Interestingly, activator protein 1 (AP1) and HNF4A had the highest number of Gene Set Enrichment Analysis–annotated target genes (Figure 3C), whereas the percentage of secreted proteins among target genes was similarly high in HNF1A and AP1 (Figure 3C). Further mapping of these transcription factor signatures revealed that HNF1A and HNF4A had the highest number of detectable targets in our plasma data, whereas only half of the secreted AP1 signatures were detectable in plasma (Figure 3D). In addition, although there was a significant correlation between the liver and plasma HNF1A and HNF4A signatures, the AP1 signature was not significant in patients with AH from the Southern California Alcoholic Hepatitis Consortium (SCAHC) Discovery cohort (Figure 3, E–G). This finding was further confirmed in the InTEAM cohort (Supplemental Figure S3, A and B), with great concordance of HNF4A and HNF1A signatures between the two cohorts of patients with severe AH (Supplemental Figure S3C) and with a set of HNF1A/HNF4A commonly and specifically regulated target genes in both cohorts (Supplemental Figure S3D). More importantly, most of the target genes of HNF4A and HNF1A were down-regulated and were related to hepatic-specific synthetic function, such as albumin, HEP2, anti–thrombin 3, serum amyloid S component, and protein C (Figure 3H). Other proteins, annotated as HNF4A-secreted targets by Gene Set

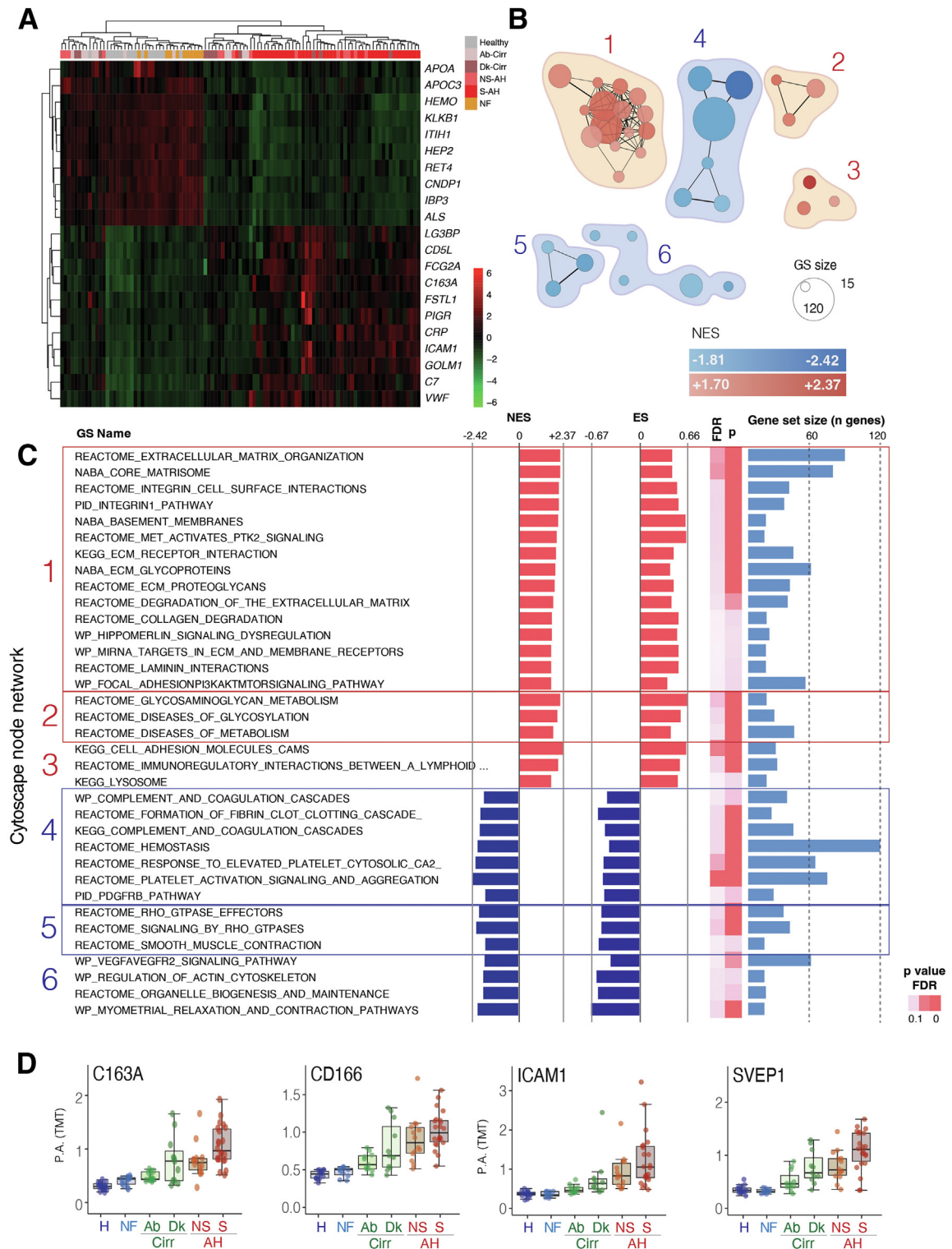


Figure 2 Protein-based pathway mapping of the alcohol-associated hepatitis (AH)—specific plasma signature. **A:** Heat map showing the top deregulated proteins (log fold change >1.7) when comparing AH with controls. Normalized protein abundance changes on plasma of healthy (H), nonalcoholic fatty liver disease (NF), abstinent cirrhotic (Ab-Cirr), recently drinking cirrhotic (Dk-Cirr), nonsevere AH (NS-AH), and severe AH (S-AH) patients are shown. **B** and **C:** Gene Set Enrichment Analysis (GSEA) was used to analyze the pathways highly relevant in differential AH transcriptome. The whole set of gene expression data, ranked by fold protein abundance between normal subjects and subjects with AH, was used. The pathways were then visualized in Cytoscape Enrichment Map software to generate the interconnected pathway network. **C:** Detailed view of top clusters of gene sets from GSEA data. Cytoscape cluster number corresponds to the ones on **B**. Vertical dotted lines indicate the gene set sizes of 60 and 120. **D:** Examples of progressively up-regulated proteins in the SCAHC cohort. ES, enrichment score; FDR, false discovery ratio; GS, gene set; NES, normalized enrichment score; *P*, *P* value; PA, protein abundance; TMT, Tandem Mass Tag.

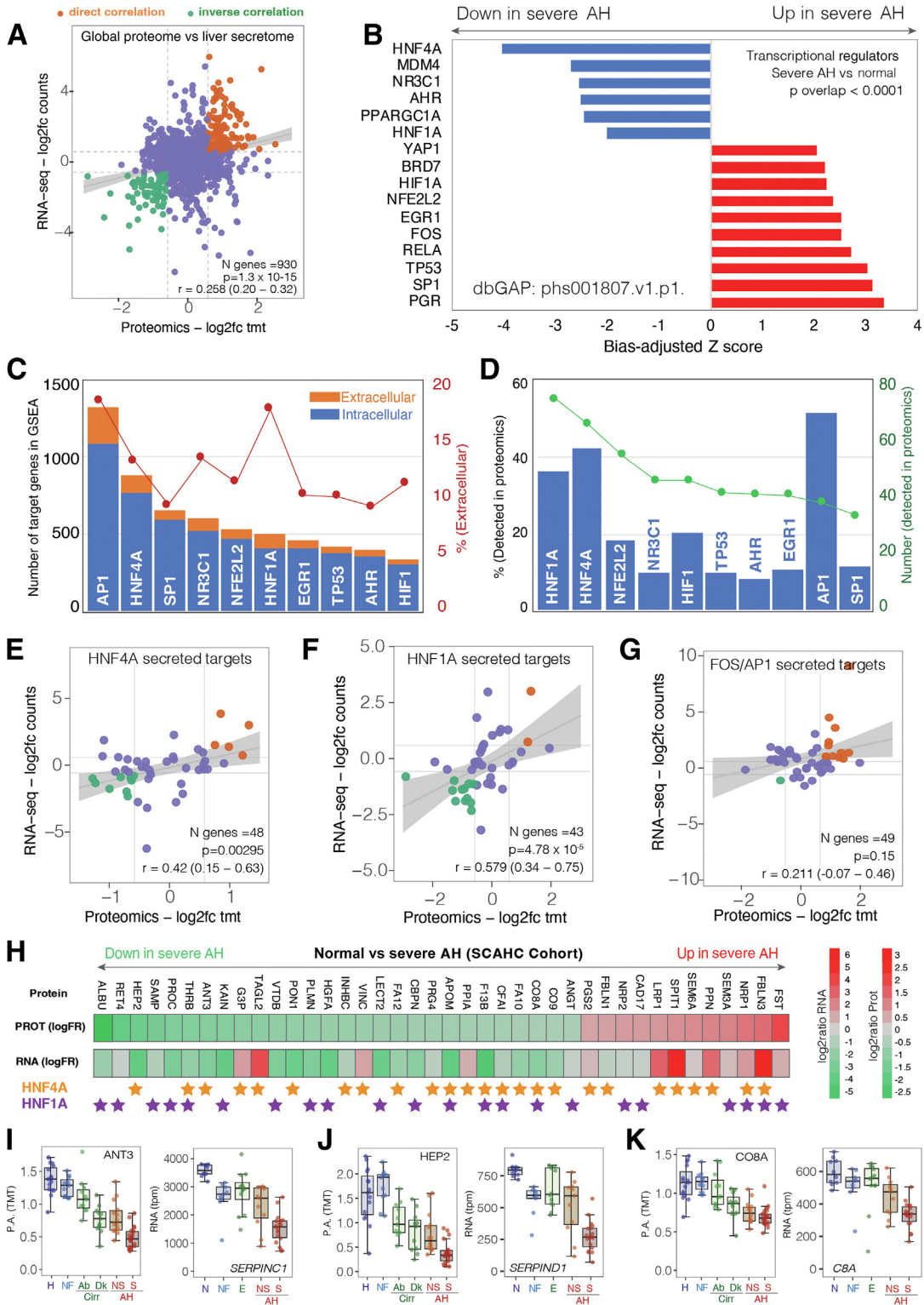


Figure 3 Patients with alcohol-associated hepatitis (AH) display a circulating liver-enriched transcription factor signature. **A:** Correlation between the relative expression of genes encoding secreted proteins in the liver and the abundance of their circulating levels. Shaded area indicates 95% CI. **B:** Transcription factor (TF) signatures in the liver transcriptome of patients with AH, when compared with normal livers. **C and D:** Characteristics of TF signatures, including the number of target genes encoding extracellular (secreted) proteins per TF (**C**) and the percentage of secreted proteins detected by proteomics (**D**). **E–G:** Correlation of the expression and the abundance of HNF4A (**E**), HNF1A (**F**), and Fos proto-oncogene, AP-1 transcription factor subunit (FOS/AP1) (**G**). Shaded areas indicate 95% CI. **H:** HNF4A and HNF1A top differentially regulated secreted target genes indicating the fold change in liver expression and in protein abundance. **I–K:** Hepatic mRNA expression and plasma protein abundance of representative HNF4A target genes anti-thrombin 3 (ANT3; **I**), heparin cofactor 2 (HEP2; **J**), and complement 8A (CO8A; **K**). Box represents the 25th and 75th percentiles, median values are represented by the lines, and error bars represent the 90th and 10th percentiles.

Enrichment Analysis, such as Kunitz-type protease inhibitor 1, an inhibitor of hepatocyte growth factor, and epidermal growth factor–containing fibulin-like extracellular matrix protein 1, were up-regulated both in liver RNA expression and plasma protein (Figure 3H). Interestingly, Kunitz-type protease inhibitor 1 and fibulin-like extracellular matrix protein 1 are strongly associated with transforming growth factor beta 1 (TGFB1) and epidermal growth factor receptor signaling, respectively, the two main pathways involved in HNF4A down-regulation in AH livers.⁹ A clear parallelism of plasma protein levels and liver RNA was shown for several HNF4A targets, such as anti–thrombin 3 (Figure 3I), HEP2 (Figure 3J), and complement 8A (Figure 3K). Overall, these results indicate that it is possible to identify blood plasma signatures of liver transcription factor activity, especially those dependent on LETFs, such as HNF4A and HNF1A. Analysis of the confirmatory cohort indicated similar results. A direct correlation of liver RNA expression and plasma protein abundance for HNF4A and HNF1A secreted targets (Supplemental Figure S3, A and B) with a complete overlap of the targets between cohorts (Supplemental Figure S3C) and a transcription factor specificity (Supplemental Figure S3D and Supplemental Table S5). However, the confirmatory cohort missed some of the hits encountered in the original cohort. Top target genes were down-regulated or up-regulated at similar levels in both discovery and confirmatory sAH cohorts, as is shown for anti–thrombin 3, HEP2, and complement 8A (Supplemental Figure S3E), and for fibulin-like extracellular matrix protein 1 and neuropilin-1 (NRP1) (Supplemental Figure S3F).

Proteome Analysis Identifies a Signature of Disease Severity in AH

Although clinical scores [such as Maddrey discriminant function, Model for End-Stage Liver Disease, Glasgow Alcoholic Hepatitis Score, or age-bilirubin-international normalized ratio-creatinine (ABIC)] have proven to be useful for deciding treatment, new equally noninvasive molecular markers of severity in the context of AH could help better understand the biology of this form of liver failure, discriminate the type of progression among patients evaluated for suspected AH, and stratify the risk of progression to liver failure in the future. Therefore, the study aimed at establishing an unbiased clinically relevant protein signature of severity in AH. As expected, the plasma proteome of patients with nsAH had fewer differently abundant proteins than severe AH (sAH) when compared with healthy or diseased control plasma samples (Figure 4A). In total, 51 proteins were changed in patients with nsAH, of which 20 were also identified in patients with sAH, revealing an expected overlap between nsAH and sAH signatures (Figure 4A and Supplemental Table S6). The abundant distribution of both sets of proteins indicated homogeneity among the differential protein abundance in the nsAH and sAH cohorts compared with healthy control, indicating similar mechanisms taking place at a higher degree along with the severity of the disease (Figure 4B). To identify protein signatures that could

potentially discriminate patients with sAH and nsAH, the study focused on the 80 discriminatory proteins that were changed in patients with sAH but not in patients with nsAH. Most of the 80 sAH-specific proteins were down-regulated when compared with healthy controls (71%) (Figure 4, C and D). As stated above, in most cases, changes in patients with nsAH represented an attenuated version of sAH changes (Figure 4, B and C). Odds ratio calculation identified a clear subset of proteins appearing most differentially abundant between sAH and nsAH (Figure 4D). Association of the plasma levels of these proteins to patients with sAH was analyzed by logistic regression when compared with nsAH. The plasma levels of clusterin, thrombin, FA9, hepatocyte growth factor α (HGFA), kallistatin, and C163A showed significant association with the sAH phenotype (Figure 4C and Supplemental Table S7).

Whether the plasma levels of these proteins could be used to discriminate between patients with severe and nonsevere AH was analyzed by plotting the receiver operating characteristic curves of these markers (Supplemental Table S8). Thrombin and HGFA showed the greatest potential in the discovery SCAHC cohort with the combination linear model providing improved discrimination (Figure 5A). These results were also validated in the InTEAM confirmatory cohort of sAH (Supplemental Figure S4, A and B). To investigate further the relationship of these targets against additional liver disease scoring functions, these targets were correlated against the Model for End-Stage Liver Disease, Child Pugh patient evaluations (Figure 5, B and C), and other clinical parameters (Supplemental Figure S5). These results indicate a robust correlation and *P* value, which was also validated in the confirmatory cohort (Supplemental Figure S4, B and C).

Discussion

This study used a sensitive liquid chromatography–tandem mass spectrometry proteomic method to identify, quantify, and compare >1500 plasma proteins from patients with AH and controls, including those with alcoholic cirrhosis, those with nonalcoholic fatty liver disease, and healthy controls. This analysis differs from previous clinical AH targeted plasma studies by providing an unbiased view of the plasma proteome signature within AH. Patients with biopsy-proven severe AH from two separate National Institute of Alcohol Abuse and Alcoholism–funded consortia, as well as multiple comparison groups, including abstinent and recently drinking alcohol-related cirrhosis were included.

Prior studies showed that systemic inflammatory response is a key event associated with multiorgan failure and early death in patients with severe AH.⁸ The molecular drivers mediating this condition are not well known. The current study showed increased circulating C163A in patients with AH. C163A is likely shed from activated monocytes and macrophages and has also been associated with several liver diseases, including viral hepatitis, nonalcoholic fatty liver disease/nonalcoholic steatohepatitis, and drug-induced liver

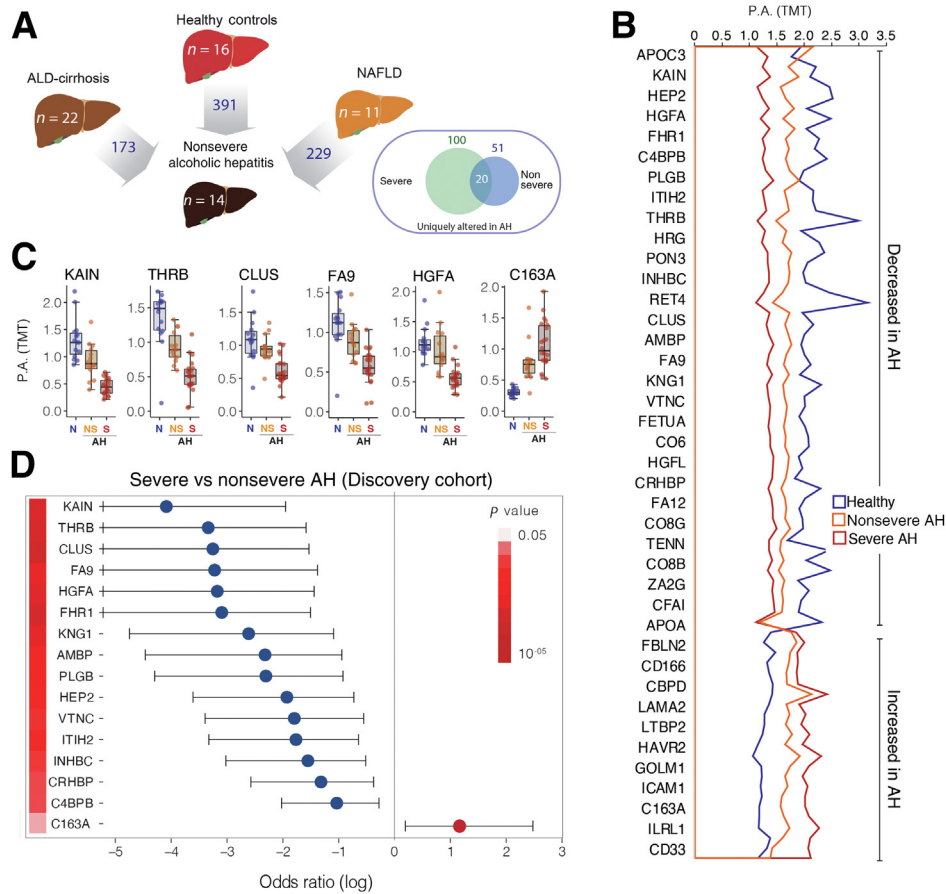


Figure 4 Key elements of the coagulation and complement system are discriminant of alcohol-associated hepatitis (AH) severity. **A:** Schematic diagram of the groups compared to obtain a plasma signature of nonsevere AH. The severe AH group was then compared with nonsevere AH, to identify markers of severity through a Venn diagram. The specific nonsevere AH signature included 51 differentially abundant proteins, whereas the specific severe AH signature included 100 plasma proteins. A total of 20 proteins were dysregulated in all patients with AH, regardless of the severity. **B:** Plasma protein abundance of nonsevere AH and severe AH discriminatory markers. **C:** Box plot of representative differentially abundant proteins when comparing severe versus nonsevere AH. Box represents the 25th and 75th percentiles, median values are represented by the lines, and error bars represent the 90th and 10th percentiles. **D:** Forest plot of odds ratios for the most discriminatory plasma proteins in severe AH versus nonsevere AH determination. P values are depicted in color heat map. ALD, alcohol-related liver disease; CLUS, clusterin; HGFA, hepatocyte growth factor α ; KAIN, kallistatin; NAFLD, nonalcoholic fatty liver disease; PA, protein abundance; THR, thrombin; TMT, Tandem Mass Tag.

injury.^{24,27–31} In addition, cell adhesion and extracellular matrix components, including intercellular adhesion molecule 1, cell adhesion molecule 1 (CADM1), CD166, and sushi, von Willebrand factor type A, EGF and pentraxin domain containing 1 (SVEP1), are also highly abundant in the systemic circulation. Although several cell surface markers, including intercellular adhesion molecule 1,^{24,32} have been investigated previously in AH, others, such as CD166, SVEP1, and CADM1, have not been associated with this disease. CD166 (alias activated leukocyte cell adhesion molecule) is involved in processes of T-cell adhesion and migration. A nonsynonymous single-nucleotide polymorphism in SVEP1 (Gln581His) has been associated to poor outcomes in sepsis,³³ and its role appears to be associated with leukocyte adhesion. Finally, CADM1 is a well-known cell adhesion molecule participating in processes of immune cell activation and migration but is also involved in the intercellular junctions in several cell types.³⁴ A recently

correlated study of proteomic and phosphoproteomic investigation of liver biopsy tissue, which overlapped with 34 of the SCAHC patients with AH,³⁵ further confirmed the tissue-specific indicators of AH-driven inflammation. Specifically, intercellular adhesion molecule 1, CD166, and SVEP1 were significantly up-regulated in the liver tissue samples among patients with AH compared with non-ALD controls, consistent with what was observed in plasma. However, C163A and CADM1 protein levels were not altered in the liver of patients with AH, possibly suggesting that the elevated plasma levels of C163A and CADM1 have additional sources of secretion other than from liver. Prospective studies should evaluate whether the expression of inflammatory biomarkers is associated with the development of extrahepatic organ damage, such as renal failure, ultimately leading to multi-organ failure and death. It is also plausible that maneuvers interacting with these mediators could have therapeutic potential in AH.

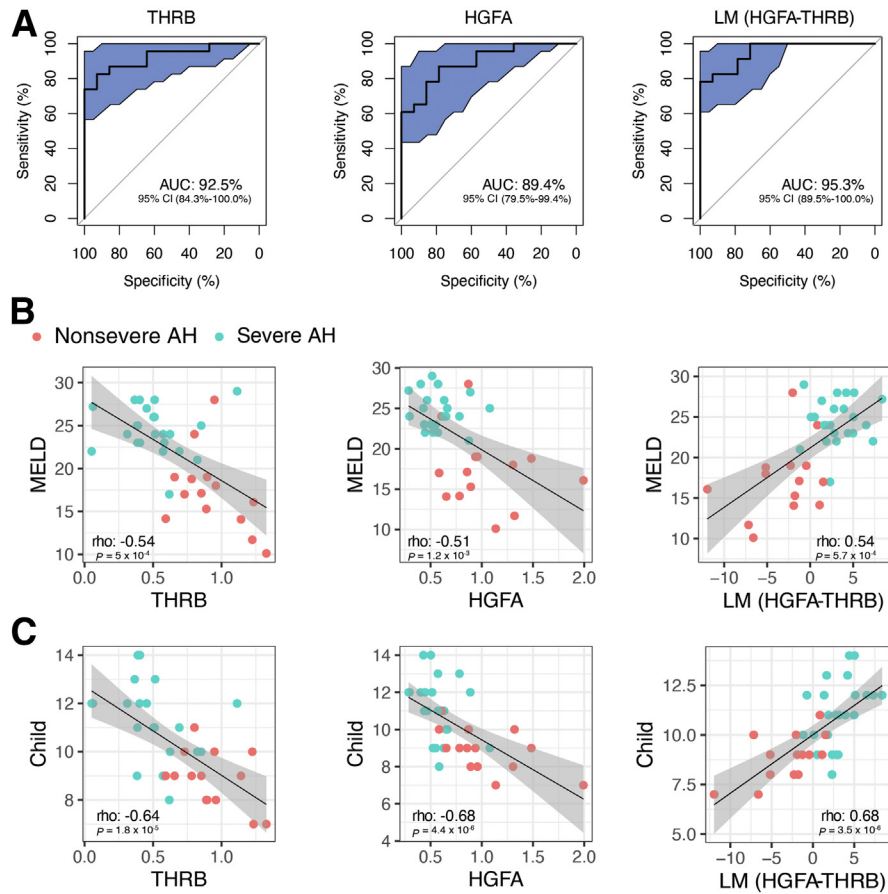


Figure 5 Receiver operating characteristic (ROC) curve and correlation of top discriminatory protein signatures. **A:** ROC curve plots of thrombin (THRb), hepatocyte growth factor α (HGFA), and a linear model using both THRb and HGFA for severity discrimination [severe alcohol-associated hepatitis (sAH) versus nonsevere alcohol-associated hepatitis (nsAH)] with the Discovery cohort. Shaded areas indicate 95% CI. **B:** Pearson correlation of within nsAH and sAH patients for discriminatory markers. **C:** Pearson correlation of discriminatory markers with patient Child Pugh score. AUC, area under the curve; MELD, Model for End-Stage Liver Disease.

Integrating the known activity of liver transcription factors and their downstream effects onto the differential protein plasma observations allowed for the identification of a proteome-based noninvasive signature of the activity of HNF4A and other companion factors, such as HNF1A. This led to the important finding that proteins reflecting LETF activity, which are master regulators of hepatocellular biological function, are potential plasma biomarkers in patients with AH. Thus, HNF4a-dependent coagulation system elements, such as anti-thrombin 3, HEP2, factors 10 and 12, or proteins belonging to the complement system, such as complement 8A, are markedly reduced in the plasma of patients with AH, especially in patients with greater disease severity. Down-regulation of these genes was also associated with severe AH stages. Similarly, proteins that are modulated by HNF1a regulating clotting cascade, such as kallistatin and protein C, were decreased in the plasma and the liver of patients with severe AH. Interestingly, other HNF1A targets essential for liver regeneration and hepatocyte function, such as hepatocyte growth factor activator (HGFA), were also down-regulated at the mRNA and protein levels. We further compared our findings on LETF target genes with the

proteomic study on liver samples.³⁵ Interestingly, in contrast with reduced protein level in plasma and down-regulation of mRNA in liver, the protein level of LETF targets in AH liver tissue appeared elevated. Such findings allude to the possible disruption of secretory mechanisms, proteasome functions, and overall protein translocation processing causing discrepancy in proteome abundance versus genomic activation. Additional possible mechanisms include regulation from liver to plasma via protein post-translational modifications. Hepatic albumin expression is regulated by HNF4a, and Tagliabracci et al³⁶ have shown that kinase Fam20A/C was responsible for albumin phosphorylation at serine82, which facilitated its secretion process. The coupled proteomic and phosphoproteomic analysis on liver samples discovered that although hepatic albumin was increased in AH, the phosphorylation of albumin at serine82 was reduced among patients with AH; thus, dysregulation of phosphorylation could lead to discrepancy between plasma and liver protein level. Non-LEFT target proteins were dysregulated in patients with severe AH.

A selected group of proteins, such as kallistatin, human serum factor H-related protein, clusterin, thrombin, FA9, HGFA, and C163A, classified the patients with AH by

disease severity, with thrombin and HGFA providing robust receiver operating characteristic evaluations. These circulating proteins represent potential biomarkers to assess liver synthetic dysfunction in AH, and a more exhaustive cross-evaluation of these markers with higher-throughput orthogonal measures to better quantify protein levels will likely generate a robust AH severity signature. Our sample and data set will allow us to measure dynamic changes in these proteins and whether changes predict the spontaneous recovery and/or response to therapy with treatment.

In conclusion, the current study used an integrative multi-omic approach to identify markers of systemic inflammation (C163A and leukocyte adhesion proteins) and hepatocellular dysregulation in patients with AH. These plasma biomarkers can be useful for diagnostic and prognostic purposes and can favor precision medicine in this patient population. Prospective longitudinal studies can be used to evaluate the performance of these biomarkers in monitoring the response to therapy. Moreover, given the biological functions of some of these proteins, it is plausible that drugs interfering with inflammatory mediators have beneficial effects by preventing multiorgan failure.

Overall, the current study had several strengths and weaknesses. The inclusion of biopsy-proven severe AH from two separate cohorts and the inclusion of multiple control groups, especially currently drinking alcoholic cirrhosis, abstinent alcoholic cirrhosis, and nonsevere AH, all of which share considerable liver pathophysiology with severe AH (eg, alcohol use, cirrhosis, and liver injury), suggests that the top candidates shown herein could be of clinical relevance. Liquid chromatography–tandem mass spectrometry has known sensitivity limits for low abundance proteins. For example, it did not detect some cytokine-related proteins that have been reported to be elevated in AH plasma using more sensitive enzyme-linked immunosorbent assay methods. Third, the interpretation of changes in plasma proteins, as they relate to pathophysiology of liver injury or to the consequence of systemic inflammatory response, will require mechanistic studies. The study applied an unbiased assessment of a broad number of plasma proteins, without prior assumptions. In summary, this study provides a robust, comprehensive, and unbiased view of plasma proteins in AH from which informed decisions can be drawn for further investigation. Specifically, it identified core sets of proteins that differentiate AH from relevant control populations, including nonsevere versus severe AH, being thus related to diagnosis. Additional studies will be needed to validate the specific protein signatures that we have identified and to assess their role in the diagnosis and prognosis of patients with AH, and for mechanistic studies of alcohol-related liver injury.

Acknowledgments

Work was performed in the Environmental Molecular Sciences Laboratory, a US Department of Energy Office of Biological and Environmental Research national scientific

user facility located at Pacific Northwest National Laboratory (Richland, WA). Pacific Northwest National Laboratory is operated by Battelle for the US Department of Energy under contract DE-AC05-76RLO 1830.

Author Contributions

J.A., J.M.J., T.R.M., and R.B. drafted the manuscript; J.A., K.K., Z.-X.L., T.M.N.-K., L.Z.D., and J.M.J. analyzed the data; J.A. performed statistical analysis; M.A.G., J.M.H., S.R.A., A.C.-S., A.S., J.A.T., R.B., T.R.M., and A.A. contributed material support; M.A.G., A.A., A.C.-S., J.A.T., R.B., T.R.M., and J.M.J. conceived and designed the study; Z.-X.L., T.M.N.-K., J.M.J., and L.Z.D. acquired data; and R.B., T.R.M., J.M.J., and R.D.S. obtained funding.

Supplemental Data

Supplemental material for this article can be found at <http://doi.org/10.1016/j.ajpath.2022.08.009>.

References

1. Shah ND, Ventura-Cots M, Abraldes JG, Alboraie M, Alfidhli A, Argemi J, et al: Alcohol-related liver disease is rarely detected at early stages compared with liver diseases of other etiologies worldwide. *Clin Gastroenterol Hepatol* 2019, 17:2320–2329.e12
2. Asrani SK, Devarbhavi H, Eaton J, Kamath PS: Burden of liver diseases in the world. *J Hepatol* 2019, 70:151–171
3. Altamirano J, Miquel R, Katoonizadeh A, Abraldes JG, Duarte-Rojo A, Louvet A, Augustin S, Mookerjee RP, Michelena J, Smyrk TC, Buob D, Leteurtre E, Rincon D, Ruiz P, Garcia-Pagan JC, Guerrero-Marquez C, Jones PD, Barritt AS, Arroyo V, Bruguera M, Banares R, Gines P, Caballeria J, Roskams T, Nevens F, Jalan R, Mathurin P, Shah VH, Bataller R: A histologic scoring system for prognosis of patients with alcoholic hepatitis. *Gastroenterology* 2014, 146:1231–1239.e1-6
4. Thursz MR, Richardson P, Allison M, Austin A, Bowers M, Day CP, Downs N, Gleeson D, MacGilchrist A, Grant A, Hood S, Masson S, McCune A, Mellor J, O'Grady J, Patch D, Ratcliffe I, Roderick P, Stanton L, Vergis N, Wright M, Ryder S, Forrest EH, STOPAH Trial: Prednisolone or pentoxifylline for alcoholic hepatitis. *N Engl J Med* 2015, 372:1619–1628
5. Louvet A, Thursz MR, Kim DJ, Labreuche J, Atkinson S, Sidhu SS, O'Grady JG, Akriviadis E, Sinakos E, Carithers RL Jr, Ramond MJ, Maddrey WC, Morgan TR, Duhamel A, Mathurin P: Corticosteroids reduce risk of death within 28 days for patients with severe alcoholic hepatitis, compared with pentoxifylline or placebo—a meta-analysis of individual data. *Gastroenterology* 2018, 155:458–468.e8
6. Lucey MR, Mathurin P, Morgan TR: Alcoholic hepatitis. *N Engl J Med* 2009, 360:2758–2769
7. Singal AK, Bataller R, Ahn J, Kamath PS, Shah VH: ACG clinical guideline: alcoholic liver disease. *Am J Gastroenterol* 2018, 113:175–194
8. Michelena J, Altamirano J, Abraldes JG, Affo S, Morales-Ibanez O, Sancho-Bru P, Dominguez M, Garcia-Pagan JC, Fernandez J, Arroyo V, Gines P, Louvet A, Mathurin P, Mehal WZ, Caballeria J, Bataller R: Systemic inflammatory response and serum lipopolysaccharide levels predict multiple organ failure and death in alcoholic hepatitis. *Hepatology* 2015, 62:762–772

9. Argemi J, Latasa MU, Atkinson SR, Blokhin IO, Massey V, Gue JP, et al: Defective HNF4alpha-dependent gene expression as a driver of hepatocellular failure in alcoholic hepatitis. *Nat Commun* 2019, 10:3126
10. Eissfeldt AJ, Halfmann PJ, Wendler JP, Kyle JE, Burnum-Johnson KE, Peralta Z, Maemura T, Walters KB, Watanabe T, Fukuyama S, Yamashita M, Jacobs JM, Kim YM, Casey CP, Stratton KG, Webb-Robertson BM, Gritsenko MA, Monroe ME, Weitz KK, Shukla AK, Tian M, Neumann G, Reed JL, van Bakel H, Metz TO, Smith RD, Waters KM, N'Jai A, Sahr F, Kawaoka Y: Multi-platform 'omics analysis of human Ebola virus disease pathogenesis. *Cell Host Microbe* 2017, 22:817–829.e8
11. Orwoll ES, Wiedrick J, Jacobs J, Baker ES, Piehowski P, Petyuk V, Gao Y, Shi T, Smith RD, Bauer DC, Cummings SR, Nielson CM, Lapidus J: Osteoporotic Fractures in Men Study Research Group: High-throughput serum proteomics for the identification of protein biomarkers of mortality in older men. *Aging Cell* 2018, 17:e12717
12. Nielson CM, Jones KS, Bouillon R, Osteoporotic Fractures in Men Research G, Chun RF, Jacobs J, Wang Y, Hewison M, Adams JS, Swanson CM, Lee CG, Vanderschueren D, Pauwels S, Prentice A, Smith RD, Shi T, Gao Y, Zmuda JM, Lapidus J, Cauley JA, Schoenmakers I, Orwoll ES: Role of assay type in determining free 25-hydroxyvitamin D levels in diverse populations. *N Engl J Med* 2016, 374:1695–1696
13. Nielson CM, Wiedrick J, Shen J, Jacobs J, Baker ES, Baraff A, Piehowski P, Lee CG, Baratt A, Petyuk V, McWeeny S, Lim JY, Bauer DC, Lane NE, Cawthon PM, Smith RD, Lapidus J, Orwoll ES; Osteoporotic Fractures in Men Study Research Group: Identification of hip BMD loss and fracture risk markers through population-based serum proteomics. *J Bone Miner Res* 2017, 32:1559–1567
14. Zhang H, Liu T, Zhang Z, Payne SH, Zhang B, McDermott JE, et al: Integrated proteogenomic characterization of human high-grade serous ovarian cancer. *Cell* 2016, 166:755–765
15. Sigdel TK, Gao Y, He J, Wang A, Nicora CD, Fillmore TL, Shi T, Webb-Robertson BJ, Smith RD, Qian WJ, Salvatierra O, Camp DG 2nd, Sarwal MM: Mining the human urine proteome for monitoring renal transplant injury. *Kidney Int* 2016, 89:1244–1252
16. Crabb DW, Bataller R, Chalasani NP, Kamath PS, Lucey M, Mathurin P, McClain C, McCullough A, Mitchell MC, Morgan TR, Nagy L, Radaeva S, Sanyal A, Shah V, Szabo G, Consortia NAH: Standard definitions and common data elements for clinical trials in patients with alcoholic hepatitis: recommendation from the NIAAA Alcoholic Hepatitis Consortia. *Gastroenterology* 2016, 150:785–790
17. Baker ES, Burnum-Johnson KE, Jacobs JM, Diamond DL, Brown RN, Ibrahim YM, Orton DJ, Piehowski PD, Purdy DE, Moore RJ, Danielson WF 3rd, Monroe ME, Crowell KL, Slys GW, Gritsenko MA, Sandoval JD, Lamarche BL, Matzke MM, Webb-Robertson BJ, Simons BC, McMahon BJ, Bhattacharya R, Perkins JD, Carithers RL Jr, Strom S, Self SG, Katze MG, Anderson GA, Smith RD: Advancing the high throughput identification of liver fibrosis protein signatures using multiplexed ion mobility spectrometry. *Mol Cell Proteomics* 2014, 13:1119–1127
18. Wang Y, Yang F, Gritsenko MA, Clauss T, Liu T, Shen Y, Monroe ME, Lopez-Ferrer D, Reno T, Moore RJ, Klemke RL, Camp DG 2nd, Smith RD: Reversed-phase chromatography with multiple fraction concatenation strategy for proteome profiling of human MCF10A cells. *Proteomics* 2011, 11:2019–2026
19. Kim S, Gupta N, Pevzner PA: Spectral probabilities and generating functions of tandem mass spectra: a strike against decoy databases. *J Proteome Res* 2008, 7:3354–3363
20. Elias JE, Gygi SP: Target-decoy search strategy for increased confidence in large-scale protein identifications by mass spectrometry. *Nat Methods* 2007, 4:207–214
21. Qian WJ, Liu T, Monroe ME, Strittmatter EF, Jacobs JM, Kangas LJ, Petritis K, Camp DG 2nd, Smith RD: Probability-based evaluation of peptide and protein identifications from tandem mass spectrometry and SEQUEST analysis: the human proteome. *J Proteome Res* 2005, 4:53–62
22. Vizcaino JA, Deutsch EW, Wang R, Csordas A, Reisinger F, Rios D, Dienes JA, Sun Z, Farrah T, Bandeira N, Binz PA, Xenarios I, Eisenacher M, Mayer G, Gatto L, Campos A, Chalkley RJ, Kraus HJ, Albar JP, Martinez-Bartolome S, Apweiler R, Omenn GS, Martens L, Jones AR, Hermjakob H: ProteomeXchange provides globally coordinated proteomics data submission and dissemination. *Nat Biotechnol* 2014, 32:223–226
23. Binder JX, Pletscher-Frankild S, Tsafou K, Stolte C, O'Donoghue SI, Schneider R, Jensen LJ: COMPARTMENTS: unification and visualization of protein subcellular localization evidence. *Database (Oxford)* 2014, 2014:bau012
24. Saha B, Tornai D, Kodys K, Adejumo A, Lowe P, McClain C, Mitchell M, McCullough A, Srinivasan D, Kroll-Desrosiers A, Barton B, Radaeva S, Szabo G: Biomarkers of macrophage activation and immune danger signals predict clinical outcomes in alcoholic hepatitis. *Hepatology* 2019, 70:1134–1149
25. Gao B, Ahmad MF, Nagy LE, Tsukamoto H: Inflammatory pathways in alcoholic steatohepatitis. *J Hepatol* 2019, 70:249–259
26. McCullough RL, McMullen MR, Sheehan MM, Poulsen KL, Roychowdhury S, Chiang DJ, Pritchard MT, Caballeria J, Nagy LE: Complement factor D protects mice from ethanol-induced inflammation and liver injury. *Am J Physiol Gastrointest Liver Physiol* 2018, 315:G66–G79
27. Mueller JL, Feeny ER, Zheng H, Misraji J, Kruger AJ, Alatrakchi N, King LY, Gelrud L, Corey KE, Chung RT: Circulating soluble CD163 is associated with steatohepatitis and advanced fibrosis in nonalcoholic fatty liver disease. *Clin Transl Gastroenterol* 2015, 6:e114
28. Siggaard CB, Kazankov K, Rodgaard-Hansen S, Moller HJ, Donnelly MC, Simpson KJ, Gronbaek H: Macrophage markers soluble CD163 and soluble mannose receptor are associated with liver injury in patients with paracetamol overdose. *Scand J Gastroenterol* 2019, 54:623–632
29. Kazankov K, Barrera F, Moller HJ, Rosso C, Bugianesi E, David E, Younes R, Esmaili S, Eslam M, McLeod D, Bibby BM, Vilstrup H, George J, Gronbaek H: The macrophage activation marker sCD163 is associated with morphological disease stages in patients with non-alcoholic fatty liver disease. *Liver Int* 2016, 36:1549–1557
30. Kazankov K, Barrera F, Moller HJ, Bibby BM, Vilstrup H, George J, Gronbaek H: Soluble CD163, a macrophage activation marker, is independently associated with fibrosis in patients with chronic viral hepatitis B and C. *Hepatology* 2014, 60:521–530
31. Sandahl TD, Gronbaek H, Moller HJ, Stoy S, Thomsen KL, Dige AK, Agnholt J, Hamilton-Dutoit S, Thiel S, Vilstrup H: Hepatic macrophage activation and the LPS pathway in patients with alcoholic hepatitis: a prospective cohort study. *Am J Gastroenterol* 2014, 109:1749–1756
32. Nagy I, Mandi Y: Serum and ascitic levels of soluble intercellular adhesion molecule-1 in patients with alcoholic liver cirrhosis: relation to biochemical markers of disease activity and alcohol intake. *Alcohol Clin Exp Res* 1996, 20:929–933
33. Nakada TA, Russell JA, Boyd JH, Thair SA, Walley KR: Identification of a nonsynonymous polymorphism in the SVEP1 gene associated with altered clinical outcomes in septic shock. *Crit Care Med* 2015, 43:101–108
34. Osawa M, Masuda M, Kusano K, Fujiwara K: Evidence for a role of platelet endothelial cell adhesion molecule-1 in endothelial cell mechanosignal transduction: is it a mechanoresponsive molecule? *J Cell Biol* 2002, 158:773–785
35. Hardesty J, Day L, Warner D, Gritsenko M, Asghar A, Stolz A, Morgan T, McClain C, Jacobs J, Kirpich I: Hepatic protein and phosphoprotein signatures of alcohol-associated cirrhosis and hepatitis. *Am J Pathol* 2022, 192:1066–1082
36. Tagliabracci VS, Wiley SE, Guo X, Kinch LN, Durrant E, Wen J, Xiao J, Cui J, Nguyen KB, Engel JL, Coon JJ, Grishin N, Pinna LA, Pagliarini DJ, Dixon JE: A single kinase generates the majority of the secreted phosphoproteome. *Cell* 2015, 161:1619–1632